

ALFABURST: A commensal search for Fast Radio Bursts with Arecibo

Griffin Foster^{1,2}★, Aris Karastergiou^{1,3,4}, Golnoosh Golpayegani^{5,6}, Mayuresh Surnis^{5,6}, Duncan R. Lorimer^{5,6}, Jayanth Chennamangalam¹, Maura McLaughlin^{5,6}, Wes Armour⁷, Jeff Cobb², David H. E. MacMahon², Xin Pei⁸, Kaustubh Rajwade⁹, Andrew P. V. Siemion^{2,10,11}, Dan Werthimer² and Chris J. Williams¹

¹University of Oxford, Sub-Department of Astrophysics, Denys Wilkinson Building, Keble Road, Oxford, OX1 3RH, United Kingdom

²Department of Astronomy, University of California, Berkeley, 501 Campbell Hall #3411, Berkeley, CA, 94720, USA

³Physics Department, University of the Western Cape, Cape Town 7535, South Africa

⁴Department of Physics and Electronics, Rhodes University, PO Box 94, Grahamstown 6140, South Africa

⁵Department of Physics and Astronomy, West Virginia University, Morgantown, WV 26505, USA

⁶Center for Gravitational Waves and Cosmology, West Virginia University, Chestnut Ridge Research Building, Morgantown, WV 26505, USA

⁷OeRC, Department of Engineering Science, University of Oxford, Keble Road, Oxford, OX1 3QG, United Kingdom

⁸Xinjiang Astronomical Observatory, Chinese Academy of Sciences, Urumqi, Xinjiang 830011, China

⁹Jodrell Bank Centre for Astrophysics, University of Manchester, Oxford Road, Manchester M13 9PL, United Kingdom

¹⁰Radboud University, Nijmegen, Netherlands

¹¹SETI Institute, Mountain View, California, USA

Accepted XXX. Received YYY; in original form ZZZ

ABSTRACT

ALFABURST has been searching for Fast Radio Bursts (FRBs) commensally with other projects using the Arecibo L-band Feed Array (ALFA) receiver at the Arecibo Observatory since July 2015. We describe the observing system and report on the non-detection of any FRBs from that time until August 2017 for a total observing time of 518 hours. With current FRB rate models, along with measurements of telescope sensitivity and beam size, we estimate that this survey probed redshifts out to about 3.4 with an effective survey volume of around 600,000 Mpc³. Based on this, we would expect, at the 99% confidence level, to see at most two FRBs. We discuss the implications of this non-detection in the context of results from other telescopes and the limitation of our search pipeline. During the survey, single pulses from 17 known pulsars were detected. We also report the discovery of a Galactic radio transient with a pulse width of 3 ms and dispersion measure of 281 pc cm⁻³, which was detected while the telescope was slewing between fields.

Key words: radio continuum: transients – methods: observational

1 INTRODUCTION

Fast Radio Bursts (FRBs) are short-duration, broad-band, dispersed pulses that are detected at radio frequencies. They are mostly classified by virtue of their dispersion being far in excess of the expected Galactic contribution. As for radio

pulsars, for FRBs, where we observe the pulse over a frequency band ranging from ν_1 to ν_2 , the resulting dispersion delay

$$\Delta t \propto \text{DM} (\nu_1^{-2} - \nu_2^{-2}), \quad (1)$$

where the Dispersion Measure (DM) is the line integral of the electron column density along the line of sight to the source.

★ E-mail: griffin.foster@physics.ox.ac.uk

Although the physical process that gives rise to FRBs is unknown, the possibility that they originate at cosmological distances, and their potential use as natural probes of large-scale structure and magneto-ionic content of the Universe makes them worthy of attention. They appear as bright sources at the telescopes on Earth, which indicates high luminosities given the implied distance. As short duration bursts, probably emanating from point-like sources, they offer the unique opportunities to probe the inter-galactic medium (IGM; Macquart & Koay 2013), as pulsars do for the Galactic interstellar medium.

Since the first reported detection (Lorimer et al. 2007), a number of surveys using a range of radio telescopes have attempted to detect further bursts. At the time of writing, 25 FRBs have been reported (for an up-to-date list, see Petroff et al. 2016). While the majority of these have been detected with the Parkes Radio Telescope at 1.4 GHz (L-band), other telescopes are making important contributions. FRB 121102 was detected in the Pulsar Arecibo L-band Feed Array (PALFA) (Spitler et al. 2014). This FRB is the only known FRB to repeat (Scholz et al. 2016). FRB 110523 was detected with the Green Bank Telescope (GBT) at 820 MHz frequencies, confirming FRBs are observable outside L-band (Masui et al. 2015). Recently, a number of very bright FRBs has been detected with UTMOST at 843 MHz (Caleb et al. 2017; Farah et al. 2017a,b) and ASKAP at 1.4 GHz (Bannister et al. 2017).

Even with the current small sample of FRBs population, it is clear that their properties vary significantly. The measured DMs range from 176 pc cm^{-3} (FRB 170827) to 2596 pc cm^{-3} (FRB 160102), with pulse widths ranging from sub-ms (unresolved) to 26 ms, and apparent flux densities covering four orders of magnitude. If the population is extra-galactic then the sky distribution is isotropic. But, there is an apparent observational disparity in the FRB event rate between high and low Galactic latitudes, possibly due to diffractive interstellar scintillation (Macquart & Johnston 2015).

Single dish telescopes have been essential to detection of FRBs and continue to be useful for population statistics. But, these telescopes provide limited localization. The unknown detection position in the primary beam, and one-off nature of most of the FRBs does also not allow precise determination of the absolute flux density or the spectral index. Only the repeater FRB 121102 has been localized using Very Long Baseline Interferometry (VLBI) (Marcote et al. 2017; Tendulkar et al. 2017). Localization is key to understanding FRBs. This requires the use of interferometric arrays with arc-second accuracy, such as MeerKAT, ASKAP, and the SKA.

Apart from localization, FRB spectra offer important clues on the nature of the emission process. Low frequency searches with LOFAR (Karastergiou et al. 2015), MWA (Tingay et al. 2015), and the GBT (Chawla et al. 2017) have reported non-detections. A limited number of FRB surveys have been above L-band frequencies. This is, in part, due to the narrowing of beam size which limits sky coverage. V-FASTR (Burke-Spolaor et al. 2016), a commensal survey on the VLBA, has reported a non-detection on observations up to 100 GHz. Law et al. (2017) ran a coordinated-in-time, multi-telescope campaign of the repeater FRB. They report non-detection of pulses at VHF, C-band, Ku-band during

periods of detected bursts in L-band and S-band. Gajjar et al. (2017) report detections of FRB121102 from 4.8 GHz (C-band). In summary, our current understanding of FRBs spectra is limited, however they appear not to follow the steep power law example of radio pulsars, and may even not be smooth and continuous with frequency.

For single dish telescopes there is a trade-off of sensitivity for survey speed. Small dishes, such as those in the ATA ‘Fly’s Eye’ survey (Siemion et al. 2012), allow for a large sky coverage, but have low sensitivity. ASKAP dishes with Phased-Array Feeds (PAFs) provide a large sky coverage with a significant enough sensitivity to detect bright FRBs. Conversely, Arecibo provides the highest sensitivity, but with a very narrow beam. The majority of FRBs have been discovered with Parkes using the multi-beam system. The high sensitivity, large number of survey hours, and increased field of view from using multiple beams all contribute to the large number of detections. Interferometric arrays such as CHIME and MeerKAT will provide both sensitivity and sky coverage. One important question relating to the nature of the FRB population is what are the statistics of source numbers versus source flux density, and whether or not the cumulative flux density distribution is consistent with a population of cosmologically distributed standard candles. To answer this question, it is particularly interesting to sample both extreme ends of the flux density axis: the brightest FRBs discovered using small telescopes in long duration and large sky-coverage surveys, as well as the weakest FRBs sampled through high-sensitivity observations with large telescopes, necessarily sacrificing survey time and sky coverage.

In this paper, we describe results from the ALFABURST survey, which has enabled high sensitivity observations to better sample the low flux density end of the population. ALFABURST makes use of the large amount of time spent by the ALFA receiver for other astronomical surveys. In Section 2, we summarize the survey parameters and observations carried out so far. A wide-feature, learned model was used to classify each dataset in order to filter out radio-frequency interference and create a priority queue for visual examination. This model and the post-processing procedures are discussed in Section 3. Although no FRBs have been found in observations carried out so far, we did detect one pulse that is consistent with an origin in the Galactic plane. This source is discussed in Section 4. We discuss the expected event rates in Section 5. Finally, in Section 6, we consider possible explanations for our non-detection of FRBs so far and speculate on future developments.

2 OBSERVATIONS

2.1 ALFABURST description

ALFABURST is an FRB search instrument which has been used to commensally observe since July 2015 with other Arecibo L-Band Feed Array (ALFA) observations at the Arecibo Observatory. This system is a component of the SETIBURST back-end (Chennamangalam et al. 2017) and uses ARTEMIS (Karastergiou et al. 2015) for automated, real-time pulse detection. We perform inline radio-frequency interference (RFI) removal, baselining using zero-DM removal (Eatough et al. 2009), and spectrum normalization

before single pulse detection. During this time period a Single Pulse Search (SPS) was performed from DM 0 to 10000 pc cm^{-3} , pulse widths from $256 \mu\text{s}$ to 16 ms (using a logarithmic decimation factor $D = 1, 2, 4, \dots, 64$), across a 56 MHz bandwidth for all 7 beams. We return to the effective DM of the search in Section 5. The gain of Arecibo allows for the most sensitive FRB search to date.

Detections above a peak signal-to-noise ratio (S/N) of 10 were recorded along with an 8.4 s dynamic spectrum window around the event. When multiple events were detected in the same time window, these events were pooled together and recorded to disk. Approximately 2.5×10^5 8.4 s datasets were recorded between July 2015 and August 2017, the vast majority of which are false detections due to Radio-frequency Interference (RFI) signals passing the real-time RFI exciser. We have detected no FRBs in our commensal survey.

2.2 Inline RFI Excision

An inline RFI exciser is implemented in the pipeline to mitigate strong RFI sources. This leads to a significant reduction in the number of false-positive detections in the dedispersion search. Individual frequency channels in a spectrum are replaced when the power exceeds a threshold T_{chan} after the spectrum is normalized to zero mean, unity standard deviation ($\mu = 0$, $\sigma = 1$). Entire spectra are also clipped when their frequency-integrated power exceeds a threshold T_{spectra} . For standard ALFABURST operation $T_{\text{chan}} = 5$ and $T_{\text{spectra}} = 10$. The RFI exciser operates on data prior to any time decimation and integration ($D = 1$).

For very bright pulses, the RFI exciser will erroneously replace channels or spectra, reducing the overall flux. For the sensitivity of the ALFA receiver, individual channels with flux greater than 2.8 Jy and, frequency-integrated flux greater than $\sim 250 \text{ mJy}$ are excised. The peaks of bright FRBs such as FRB 150807 and FRB 170827 would be significantly clipped by the exciser. But, the edges of the pulse would not. Both of these FRBs would still be detected at a significant peak S/N. All previously reported FRBs would be detected with ALFABURST at high peak S/N even if partially clipped.

The zero-DM removal and spectral replacement affects low-DM pulses. For reference, the minimum DM before the total dispersive delay across the band is equal to a time sample is $\text{DM} = 1.8 \text{ pc cm}^{-3}$ for the typical ALFABURST observing band (using Eq. 5.1 of Lorimer & Kramer (2004)). The minimum DM before the dispersive delay within a single channel equals the sampling time (also known as the diagonal DM) is $\text{DM} = 976 \text{ pc cm}^{-3}$. Single pulses from low-DM pulsars such as B0834+06 are often clipped by the exciser, but are still detected at significant peak S/N (see Table 1). As ALFABURST is focused on detecting high-DM pulses, spectral replacement does not affect the survey sensitivity.

2.3 Single Pulse Search Verification

The PALFA survey schedule includes regular observations of known pulsars to verify their data analysis pipeline. This provides a consistent verification of our SPS to detect dispersed pulses. As the PALFA survey is targeted at the Galactic

PSR	S_{1400} (mJy)	DM_{cat} pc cm^{-3}	DM_{obs} pc cm^{-3}	N_pulses	S/N _{max}
B0525+21	9.0	50.87	50	1	72.3
B0540+23	9.0	77.70	77	1	11.7
B0611+22	2.2	96.91	101	5192	48.8
J0631+1036	0.9	125.36	125	7	10.2
B0834+06	4.0	12.86	9	223	35.0
B1133+16	32.0	4.84	7	291	15.5
B1737+13	3.9	48.67	46	1880	49.4
B1859+03	4.2	402.08	402	2	20.4
B1900+01	5.5	245.17	246	151	35.4
J1908+0457	0.9	360.00	352	3	12.9
J1908+0500	0.8	201.42	202	160	18.5
J1910+0728	0.9	283.70	288	2	10.2
J1913+0904	0.2	95.30	97	1524	44.7
B1913+10	1.3	241.69	245	2	16.1
B1933+16	42.0	158.52	154	10	30.5
B1937+24	*	142.88	146	37	24.6
B2002+31	1.8	234.82	250	4	27.6

Table 1. Parameters for known pulsars detected in the ALFABURST survey. The columns from left to right are, pulsar name, mean flux density at 1400 MHz, catalog DM, observed DM of the strongest pulse, number of detected single-pulses, and maximum single-pulse S/N. The mean flux density at 1400 MHz and catalog DM were obtained from the ATNF pulsar catalog (version 1.56).

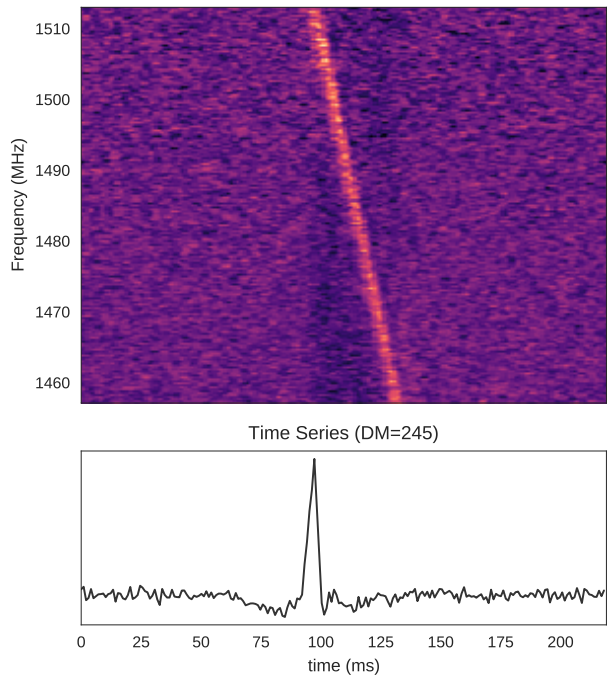


Figure 1. Detection of a single pulse from PSR B1900+01 ($\text{DM} = 245 \text{ pc cm}^{-3}$). The baseline dip before and after the pulse is due to zero-DM removal (Eatough et al. 2009).

plane, a number of high DM pulsars were observed. Single pulses from B1859+03 ($\text{DM} = 402$), B1900+01 ($\text{DM} = 245$) (Figure 1), B2002+31 ($\text{DM} = 234$), B1933+16 ($\text{DM} = 158$), among others were detected. Table 1 lists the parameters for the known pulsars detected by the SPS.

2.4 Survey Coverage

Since ALFABURST was installed, the majority of ALFA observation time is allocated for the AGES (Auld et al. 2006) and PALFA (Cordes et al. 2006) surveys (Figure 2). The AGES survey pointings are off the Galactic Plane, which is ideal for FRB surveys.. PALFA is a pulsar search survey with pointings near the Galactic Plane. These lines of sight can introduce significant dispersion due to the Interstellar Medium (ISM). We search out to a DM of 10^4 cm $^{-3}$ pc which is well beyond the maximum Galactic dispersion, but within the technical capabilities of our system.

Approximately 65% of the ALFABURST survey time has been in pointings out of the Galactic Plane ($|b| > 5^\circ$). These pointings are primarily from the ongoing AGES survey. Pointings in the plane are primarily from the PALFA survey. The PALFA survey detected the repeating FRB FRB121102 (Spitler et al. 2014), the only FRB detected with Arecibo thus far. As ALFABURST has been running commensally with the PALFA survey since 2015 these two back-ends act as independent single-pulse search pipelines, useful for detection verification. Since the beginning of ALFABURST observations no FRBs have been reported by PALFA. No follow-up observations of FRB 121102 have been conducted using ALFA.

2.5 Observing Time

From the beginning of July 2015 to the end of April 2017 ALFA has been used for approximately 1400 hours of observing, with all seven beams functional. Due to pipeline development and hardware reliability, ALFABURST was active and functional for, on average, 322 hours per beam. The current system is set up to be reliably in use for all beams any time ALFA is active and in the correct receiver turret position. Since April 2017 this stable version of the pipeline has run for an additional 196 hours. This has resulted in a total of 518 hours of processed observing time since ALFABURST began commensal observations.

3 EVENT CLASSIFICATION STRATEGY

The significant DM trial range, variety of RFI events, and commensal nature of the survey, leads to a large number of false detections. Approximately 2×10^5 unique 8.4 s datasets were recorded with at least one detection above the minimum peak S/N threshold of 10. In order to reduce the number of events we need to visually inspect we have developed a prioritizer model based on a trained probabilistic classifier. The use of trained classifier models is becoming a common post-processing technique in FRB surveys (Wagstaff et al. 2016) in order to manage the large number of detected events. Our model can be found in the survey git repository¹.

Building the model involved inspecting and labelling a sample of the events. We used a sample set of approximately 15,000 event windows. For each event window, a diagnostic plot was generated which contained the original dynamic

Class ID	N_{events}	Description
1	151	Unclipped low-level RFI
2	4159	Wide-band, duration > 1 second clipped RFI (2016+)
3	1898	Wide-band, duration < 1 second clipped RFI (2016+)
4	448	Wide-band, short duration clipped RFI (2015)
5	617	Sharp bandpass transition
6	4649	Wide-band, bursty, clipped RFI (2015)
7	863	Error in spectra capture or replacement
8	1594	Systematic int/float overflow
9	691	Astrophysical pulse or unknown event
Total	15070	

Table 2. Event classes and distribution from the sample of labelled events used to train the priority classifier model.

spectrum, the dedispersed dynamic spectrum of the S/N-maximized DM, along with a frequency collapsed time series of the detection. During figure generation 409 features were also computed to be used in the model. These features include statistics such as the number of triggers in the event window, the DM range of these triggers, and the median, mean, and standard deviation of a coarse pixelization of the dynamic spectrum (4 \times 16) and S/N maximized dedispersed time series (16 segments). A complete list of the features can be found in the survey git repository. These raw features were reduced during model pre-processing to 398 features.

In order to build a classifier model using the derived event statistics, a sample of events were visually inspected and labelled into 8 classes of RFI, systematic effects, and astrophysical source (pulsars) (Table 2). These heuristic classes were based on multiple, iterative inspections of the sampled events. A simple binary astrophysical classifier of events leads to a poor model because the types of events which are non-astrophysical take on a variety of forms.

The class distribution is time-dependent as the detection pipeline has been updated, the RFI environment has changed, and the telescope observing schedule has changed over the time the survey has run. Classes 2 and 3 occur after the inline RFI exciser was improved in 2016. Whereas classes 4 and 6 are events that occur with the original RFI exciser. Because the ALFABURST is operating in commensal mode, the band can unexpectedly be changed due to a change in the observing frequency, these event windows are labelled as class 5 events. Class 7 and 8 are due to packet loss and incorrect digital gain settings. We found that class 8 events can be removed simply by checking for overflow values in the spectra, and therefore this class is dropped before building a classifier model.

Pulses from known pulsars were used as a proxy class for the FRB class. The number of astrophysical pulse detections was low compared to the total number of false-positive detections. It was necessary to use a large number of classes as RFI and systematic effects took on a variety of forms. This had the additional effect of balancing out the number of events in each class, making model training more robust.

These features along with the labels were used to build a random forest probabilistic classifier model (Ho 1995; Breiman 2001) using the `scikit-learn` package (Pedregosa et al. 2011). This model is then used to probabilistically predict which class belongs to an unlabelled data set. A one vs.

¹ <https://github.com/griffinfoster/alfaburst-survey>

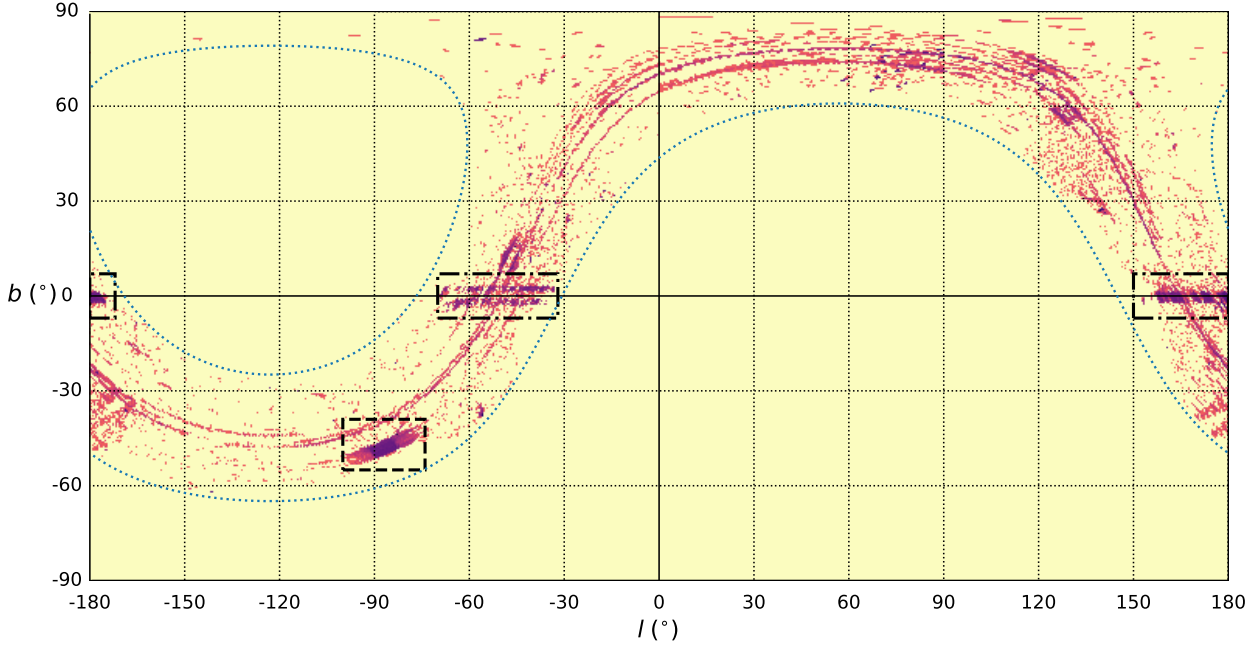


Figure 2. Sky coverage during ALFA usage between July 2015 and June 2017, shown in a Cartesian projection in Galactic coordinates along with declination pointing limits (blue dashed). Color represents total time pointing in a log scale. The majority of ALFA usage during this time was for the PALFA survey along the Galactic Plane (dot-dashed boxes) and the AGES survey (dashed box). The S-shaped arcs across the plot are due to fixed pointings in local azimuth and altitude.

the rest multi-class classifier strategy was used for training. Before training, the features of the labelled data sets were median removed and standard deviation normalized using an interquartile robust scaler. A random forest of 80 trees and 20 random features per node split was found to produce the best score in a hyper-parameter grid search using a log-loss scoring metric. During training and hyper-parameter optimization a stratified k-fold cross-validation (3 splits) (Kohavi 1995) procedure was used.

The trained model is successful at predicting the majority of the astrophysical events to be astrophysical with high probability, as shown in the confusion matrix (Figure 3) when using 75% of the labelled events for training, and 25% for testing. Of the non-astrophysical events, only 13 events were misclassified as being likely astrophysical. A reasonably small number of false-positive events to inspect. But, of the 163 astrophysical pulses in the testing set, 6 events were misclassified. This is a more serious issue as we would like to minimize the number of false-negative events for astrophysical event windows.

In searching for FRBs we are inclined to allow for a large number of false-positive events (detection due to RFI or systematics) as long as there are no false-negative events (pulses classified as RFI), i.e. a high recall for astrophysical pulses. But, the confusion matrix is computed based on a discrete class classification. The probabilistic predictions of all the astrophysical pulses to be of the astrophysical class in the test set are all above 0.25 (Figure 4), while 20 events are reported as false-positive for class 9 above this probability. We use this threshold to select the top candidates from the

Predicted Label ID	1	2	3	4	5	6	7	8	9
True Label ID	1	6	3	13	4	0	4	2	2
1	1034	1	14	0	12	4	2	0	0
2	0	28	424	0	6	11	0	2	2
3	0	0	1	74	1	31	0	0	0
4	0	12	8	2	101	13	0	0	0
5	1	5	14	7	3	1138	1	2	0
6	0	5	0	2	0	0	192	0	0
7	0	3	5	0	1	4	0	0	157
9	0	0	0	0	0	0	0	0	0

Figure 3. Confusion matrix of labelled testing data set after training the random forest model with the labelled training data set.

survey. The events are sorted into a priority queue based on the probability the event is astrophysical.

Using a probabilistic multi-label classifier allows us to prioritize the order and amount of time we spend on exam-

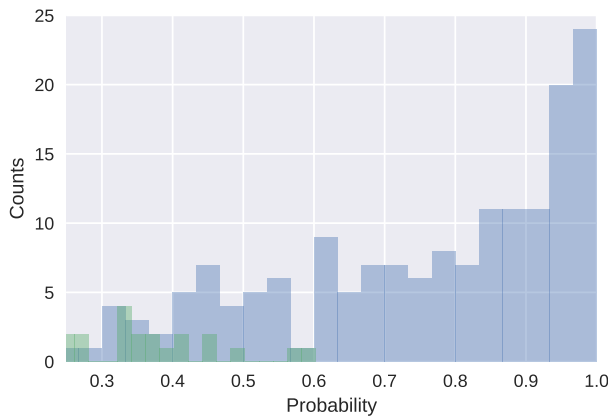


Figure 4. Histogram of the probability that a given astrophysical event (class 9, blue) and all other classes (green) is predicted to be an astrophysical event using our probabilistic classifier model.

ining event datasets. Those with high probability of belonging to a single class can be examined as a group quickly. Datasets which fall into multiple classes are examined more thoroughly, they are labelled by hand, and the set of features extracted during the figure generation process is refined to further differentiate classes. This model building, prioritizing, and examination process was iterated on multiple times to improve the classifier. We continue to iterate on this model and will use it for future prioritization of examining events.

We have not used the classifier model directly in our pipeline as the black-box nature of the model can lead to misclassification, rather we have used it to create a priority queue. We have also used our classifier model as a data exploration tool to add and refine procedural filters to the data. An output of the random forest model is the sort the features by 'importance' for classification. For example, the most important feature for correctly classifying a class 1 event (long duration replaced RFI) was the length of the longest period of the dynamic spectrum with a derivative of zero. This makes sense, as wideband RFI is replaced by a mean-zero noise spectrum. The most important features for correctly predicting an astrophysical pulse were the statistics from coarse pixelization of the dedispersed time series. This can be attributed to the detection of a high S/N event in an otherwise noisy time series.

Understanding the feature importance has led to the development of a number of simple filters to reduce the number of false-positive detections without relying on the classifier model. Data sets were cut if any of the following criteria were met:

- The maximum DM of events was less than $50 \text{ cm}^{-3} \text{ pc}$.
- Given the optimal dispersion measure, DM_{opt} , obtained from the S/N-maximized DM trial, if the DM range exceeds $(0.5 \times \text{DM}_{\text{opt}}, 1.5 \times \text{DM}_{\text{opt}})$, then the event is due to long duration RFI.
- More than 50% of the spectra were replaced in the dataset.
- Any values in the dataset exceed the `int32` maximum value. These are class 8 events, and due to errors in receiving packets.

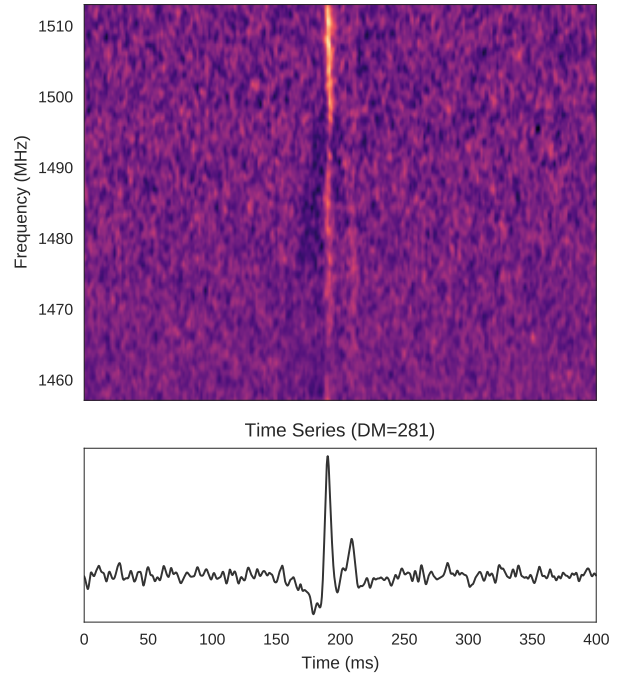


Figure 5. A broad band pulse (S/N maximized at $\text{DM} = 281 \text{ pc cm}^{-3}$) detected in beam 5 while the telescope was slewing during a PALFA observation. There is no known source which has been associated with this detection. As the observation was in the Galactic Plane it is likely Galactic in origin.

These filters were applied to each dataset in post-processing to reduce the number of datasets to approximately 30,000. The windows were sorted by S/N, and the top S/N events were examined first. During this process all datasets were labelled. Astrophysical events were identified based on the beam ID and pointing information.

4 THE EVENT OF 2017, JUNE 18

Though we report no detection of FRBs in the first two years of observations with ALFABURST we have made an initial detection of an as yet unknown broad-band (within our band) pulse (Figure 5) at a peak S/N of 18. The peak S/N is maximized by dedispersion using a DM of 281 pc cm^{-3} and time decimation factor 8. The main pulse width is approximately 3 ms. The pulse occurred in beam 5, and there were no other detections in the other beams at the time.

The pulse is made up of two clear components, with the secondary pulse arriving approximately 20 ms after the primary pulse, as seen in the dynamic spectrum (Figure 5). In DM-time space the event is compact, consistent with a ν^{-2} dispersion relation (Figure 6), though such a fit has large error bars due to the small fractional bandwidth that is processed with ALFABURST.

The detection occurred at 04:56:16 UT on 2017, June 18 (MJD 57922) during a PALFA observing run. The event was not seen by the PALFA collaboration as it occurred when the telescope was slewing between fields and the PALFA spectrometers were not running. This is the first known detection of a transient, broad-band pulse using ALFA dur-

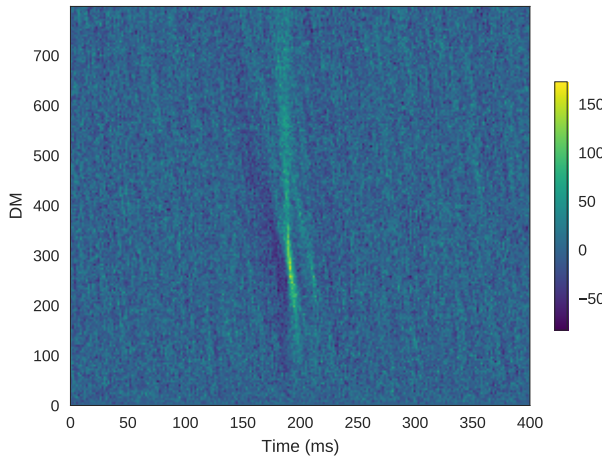


Figure 6. DM-time plot of the 2017 June 18 pulse. The pulse is compact in DM-time space, consistent with an astrophysical event. The secondary pulse 20 ms after the primary pulse causes the intensity to be slightly elongated to higher trial DMs.

ing such a slew. However, this makes it challenging to determine the accurate source position. Pointing information from Arecibo is reported every second. During the detection the pointing was changing by approximately 5' per second in right ascension 2' per second in declination. This rate gives us a conservative estimate of the error in pointing at the time the pulse was detected. Based on the time stamp of the pulse and the pointing data the pulse occurred when beam 5 of ALFA was pointing at right ascension: 18 h 45 m 10 ± 20 s, and declination: $+00^\circ 38 \pm 2'$ (Galactic coordinates $l: 32.78 \pm 0.05^\circ$, $b: +1.68 \pm 0.05^\circ$).

This beam 5 pointing is close to the Galactic plane in the first quadrant. The DM distance estimated from the NE2001 model (Cordes & Lazio 2002) is approximately 6 kpc, which is well within the Galaxy. The maximum Galactic contribution along this line of sight would produce a DM of ~ 800 pc cm $^{-3}$. A search of the ATNF pulsar database² (Manchester et al. 2005), Rotating Radio Transient (RRAT) catalog³, and recent PALFA discoveries⁴ revealed no known source with a DM near 281 pc cm $^{-3}$ within a degree of the pointing.

As the telescope was slewing at the time, the source was only in the primary lobe for a fraction of a second (assuming it was in the primary lobe and not a side lobe). A source on the edge of the Full-Width at Half-Maximum (FWHM) beam would transit the beam in a maximum of 500 ms for the slew rate of the telescope (at the ALFABURST observing frequency this corresponds to a dispersed pulse with a maximum DM of 3500 pc cm $^{-3}$). It could therefore be a RRAT which we serendipitously detected at the correct moment, or it could be an individual pulse from a pulsar. This event is similar to FRB010621 (Keane et al. 2011) which is likely of galactic origin (Bannister & Madsen 2014). Keane et al. (2012) suggest FRB010621 is due to pulsar giant pulse

or annihilating black holes. The second component would seem to rule out the latter interpretation in this instance. This region has been previously surveyed with PALFA and the Parkes Multi-beam Survey (Manchester et al. 2001) with no significant detection of a pulsar at this DM.

The pulse appears brighter at higher frequencies, which could be due to scintillation. Another reason for this frequency-dependent structure is that the pointing of the telescope is changing during the total dispersion time of the pulse within the observed band. As the pointing moves, the corresponding telescope gain also changes. There was a higher beam gain at the beginning of the pulse compared to the end of the pulse, inducing a frequency-dependent gain response due to the beam, also known as *spectral colorization*. A more detailed analysis of this event and the results of follow-up observations, will be presented elsewhere.

5 EXPECTED FRB EVENTS

The currently known 25 FRBs vary significantly in DM, pulse width, and flux density. Despite this, we assume a simple model to derive an expected event rate with our survey⁵. We use a model (see equation 9 of Lorimer et al. 2013) which assumes FRB sources are standard candles with a fixed spectral index, uniformly distributed in co-moving volume. The event rates in this model have been updated to the event rates reported in Crawford et al. (2016). For an observed pulse of typical width 4 ms (see below), these event rates are in the range 1100–7000 bursts per sky per day, where the range indicates statistical errors for the 99% credible region.

Taking advantage of the large forward gain of Arecibo, we account for the sensitivity of the 7 ALFA beams out to the outer edge of the first side lobe. In practice we do this by splitting the beam and first side lobe into shells of progressively lower gain but larger sky coverage, and integrate to obtain the totals. An ALFA beam is approximately 3.8' \times 3.3' at FWHM across the band. The ALFA beam is known to be relatively fixed in size across the band due to the optics (Heiles 2004). Given the average observing time per beam of 518 hours this results in a survey coverage of ~ 10 deg 2 hours when accounting for all 7 beams. This is a small survey coverage compared to most other FRB surveys, primarily due to the narrow beam size of Arecibo. The combined Parkes multi-beam surveys have a total of 8231 observation hours (Crawford et al. 2016), and a FWHM survey metric of ~ 4500 deg 2 hours. ALFABURST does not compete with other surveys on sky coverage, rather it competes on sensitivity. This results in probing a greater redshift range than for Parkes. Using Equation 6 of Karastergiou et al. (2015), a single-pulse-search pipeline is sensitive to pulses with a minimum flux density

$$S_{\min} = \text{SEFD} \frac{S/N_{\min}}{\sqrt{D \Delta \tau \Delta \nu}} \quad (2)$$

which is a function of the telescope System Equivalent Flux Density (SEFD), the minimum S/N detection level S/N_{\min}

² <http://www.atnf.csiro.au/people/pulsar/psrcat>

³ <http://astro.phys.wvu.edu/rratalog>

⁴ <http://www.naic.edu/~palfa/newpulsars/>

⁵ Jupyter notebooks used to carry out this work are freely available and are hosted at <https://github.com/griffinfoster/alfaburst-initial-survey>

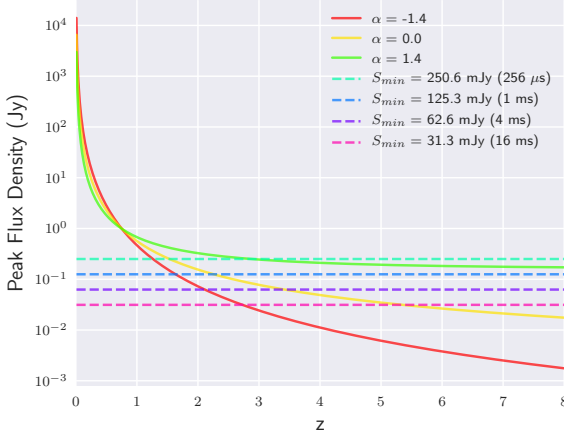


Figure 7. Sensitivity of the ALFABURST search pipeline (dashed) to FRB pulses assuming a standard candle model using different spectral index models (solid).

and the decimation factor D compared to the native instrumental time resolution τ , this comes from the search pipeline which averages together spectra to search for scattered pulses. ALFABURST has a native resolution of $\Delta\tau = 256\ \mu\text{s}$, effective bandwidth $\Delta\nu = 56\text{MHz}$, and $\text{S/N}_{min} = 10$. The FWHM SEFD of the ALFA receiver is approximately 3 Jy across the band for all beams.

The SPS pipeline is configured to search for pulses from $256\ \mu\text{s}$ to $16\ \text{ms}$. Considering only the main beam lobe, a perfect matched filter would result in a sensitivity to pulses with a minimum frequency-averaged flux of $S_{256\mu\text{s}} = 250\ \text{mJy}$ to $S_{16\ \text{ms}} = 31\ \text{mJy}$ (Karastergiou et al. 2015). Figure 7 shows the peak flux density of using the standard candle FRB model as a function of source redshift for different model spectral indices. The dashed lines of constant flux show the sensitivity of the ALFABURST search pipeline to pulses of different widths. Assuming a positive spectral index model ($\alpha = 1.4$) results in a sensitivity out to the maximum redshift/DM for pulses with widths of at least $1\ \text{ms}$. A flat spectral index model results in sensitivity from $z \sim 1.5$ ($256\ \mu\text{s}$) out to $z \sim 5$ ($16\ \text{ms}$) depending on pulse width. A negative spectral index model ($\alpha \sim -1.4$) limits the survey to $z < 3$ for all pulse widths.

If we assume a simple model of $\alpha = 0$ as we have limited information about the source spectral index, and a pulse width of $4\ \text{ms}$ as that is an approximate median pulse width of reported FRBs, then this results in a maximum redshift of $z = 3.4$ (a co-moving distance of $6.8\ \text{Gpc}$) and a survey volume of $6 \times 10^5\ \text{Mpc}^3$ when using all 7 ALFA beams. The number of galaxies sampled in this volume is 6×10^3 assuming a constant galaxy number density of 10^{-2} per Mpc^3 . The volumetric event rate from Thornton et al. (2013), is stated to be $R_{\text{FRB}} = 10^{-3}$ FRBs per galaxy per year. Adopting the more realistic lower rates found by Crawford et al. (2016) based on a larger sample of discoveries, we adopt R_{FRB} to be in the range 1.1×10^{-4} — 7.0×10^{-4} FRBs per galaxy per year. With these assumptions, we do not expect any FRB detections based on the current observation time. We note once again that the areal coverage used in this calculation

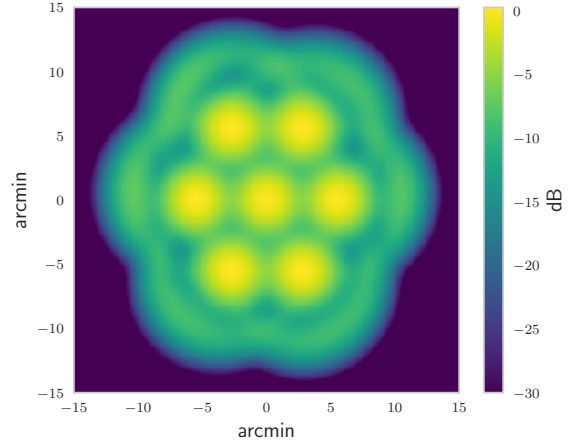


Figure 8. Primary and first side lobe model of the AFLA receiver in decibels, cut-off at $-30\ \text{dB}$. The first side lobe peak at around $-9\ \text{dB}$.

is only based on the sensitivity and size of the main beam lobe.

As mentioned above, it is worth also taking into account the entire first side lobes of the beams as Arecibo would be sensitive to detect most previous FRBs in these. Using the parameterized ALFA beam model (Figure 8) (Heiles 2004) we can compute the FRB survey metric and expected rates as a function of beam sensitivity. The first side lobes peak at around $-10\ \text{dB}$ and provide a significant increase in sky coverage compared to just the primary lobes.

The total survey metric can be computed as a function of the beam sensitivity by integrating over the beam (Figure 9). We convert the beam model to units of Jy by assuming that the $-3\ \text{dB}$ point corresponds to the FWHM SEFD of 3 Jy. The survey metric increases to approximately $26\ \text{deg}^2\ \text{hours}$ by including more of the primary beam beyond the FWHM point. The steep further increase in the survey metric seen in Figure 9 arises from including the first side lobes. The long tail comes from the residual sensitivity by integrating over the remaining beam. The beam model and polynomial fits to the survey metric curves are included in the event rate notebooks.

The survey volume is significantly increased by including a large portion of the beam. It is not possible to put together a figure similar to Figure 7 when considering the full beam. It is however possible, under the assumption of flat intrinsic FRB spectra, to compute the maximum redshift as a function of beam size and sensitivity. Plotting the survey metric as a function of maximum redshift (Figure 10) shows how the full beam model increases the survey metric as a function of redshift. The total survey volume is computed by integrating over redshift. Including additional ALFA side lobes beyond the first side lobes, results in minimal increase in the survey volume.

The integrated survey volume out to the first side lobe is $5.2 \times 10^6\ \text{Mpc}^3$. The expected number of FRBs in the survey is $0\text{--}2$ when using the galaxy number density and range of R_{FRB} stated above. Though this event rate is more complex to model, it attempts to provide a more realistic assessment

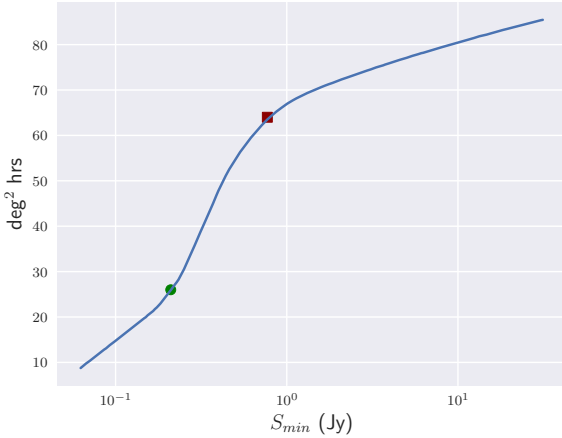


Figure 9. Survey metric as a function of the ALFA receiver minimum sensitivity using the ALFA primary and first side lobes. The -9 dB point (green circle) which is the beginning of the first side lobe sensitivity and -12 dB point (red square) which is the FWHM of the first side lobe are marked.

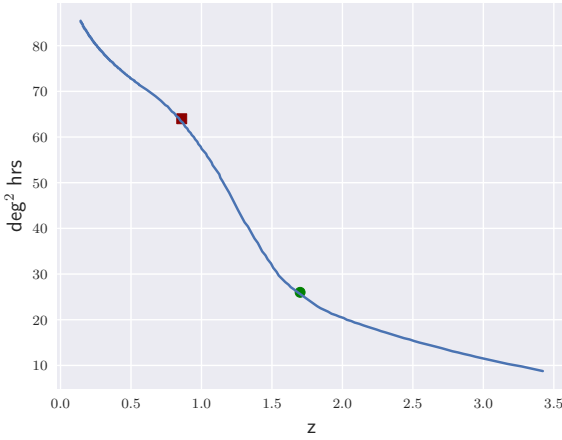


Figure 10. Survey metric as a function of redshift using the standard candle model with a flat spectral index ($\alpha = 0$) and pulse width of 4 ms. The bump out to $z = 1.5$ is due to the including the ALFA first side lobes. Markers indicate the -9 dB (green circle) and -12 dB (red square) of the ALFA beam.

of the expected detection rates based on the apparent flux of previously reported FRBs and a flat spectral index.

Figure 11 shows the ALFABURST sensitivity based on pulse width and peak flux, assuming detection at boresight. The ALFABURST sensitivity region (purple) indicates the survey would be able to detect all previously reported FRBs. Bright FRBs such as FRB150807 and FRB170827 would be partially clipped by the inline RFI exciser (Section 2.2), but they would still be detected at a high peak S/N. Additionally, in a multiple beam system a bright FRB would be picked up at a lower flux in the side lobes of nearby beams. Recent detections with UTMOST (Caleb et al. 2017; Farah et al. 2017a,b) indicate that the parameter space in pulse width

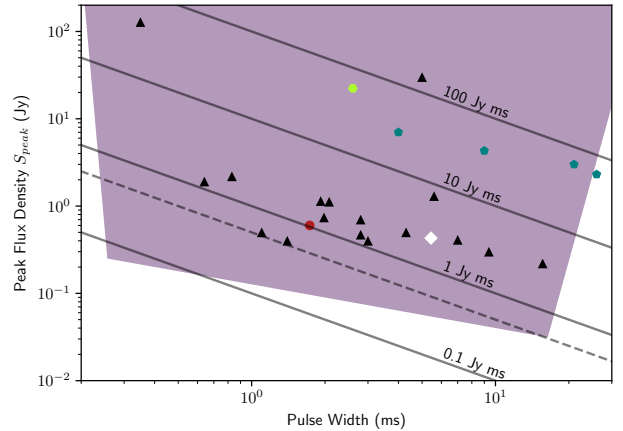


Figure 11. ALFABURST single pulse sensitivity (purple region). Previously detected FRBs from Parkes (black triangle), GBT (red circle), Arecibo (white diamond), UTMOST (teal pentagon), and ASKAP (yellow-green hexagon) are plotted for reference. Line of constant fluence (solid) are plotted for reference. The fluence completeness (dashed) is 0.5 Jy ms out to pulse widths of 16 ms.

should be extended. FRB170827 has a measured pulse width of 26 ms. Currently the pipeline decimates in time out to 16 ms. The pipeline is still sensitive to wider pulses, but at a loss in S/N as indicated in the slope on the right side of the shaded region of Figure 11. Similarly, the left side of the region is sloped as ALFABURST is sensitive to bright pulses with widths narrower than 256 μ s.

The fluence completeness of the survey (Keane & Petroff 2015) is determined by the minimum detectable fluence at the maximum sampled pulse width in the survey. ALFABURST has a fluence completeness of 0.5 Jy ms up to a pulse width of 16 ms (Figure 11). All previously reported FRBs are within this completeness sample except FRB160317 and FRB170827.

6 DISCUSSION

In addition to the small searched volume, there may be other factors contributing to our non-detection of FRBs with the ALFABURST survey. We derived an expected event rate based on the telescope sensitivity, observing time, and a standard candle model (Lorimer et al. 2013) where the rate of FRBs per host galaxy is independent of redshift. This is a simple model based on updates to the empirical event rates from detections in the High Time Resolution Universe (HTRU) survey (Thornton et al. 2013) by Crawford et al. (2016), and assumes that FRBs are singular events. All of these assumptions are subject to uncertainty. As shown by recent statistical studies of the Parkes FRBs, there is growing evidence that they are not standard candles, and their event rate is redshift dependent (Caleb et al. 2016; Rane 2017). In addition, the recent detections of bright, high-DM FRBs with ASKAP (Bannister et al. 2017) and UTMOST (Caleb et al. 2017; Farah et al. 2017a) also call into question the assumption that FRBs are standard candles. The repeating nature of FRB121102 (Spitler et al. 2016) indicates that there could be multiple classes of FRB progenitors, or

this standard candle model does not accurately model event rates. The fact that our simple estimate of 0–2 detections so far is broadly consistent with our actual null detection indicates that our results are not highly sensitive to these assumptions, but that further ALFABURST observations will begin to probe the variety of currently highly uncertain features of the FRB population. We discuss these issues, and other potentially relevant factors, further below.

The limited processing bandwidth of ALFABURST may be a cause of the survey non-detection. Multiple detected FRBs show apparent scintillation and steep spectral indices. It is not possible to differentiate between an apparent spectral index induced by the beam or an absolute spectral index from the source. The localization and repeated detections of FRB121102, however, show there is significant spectral variation, either intrinsic to the source or due to the intervening medium. Other FRBs show frequency-dependent structure which could be due to beam colorization, intrinsic structure, or due to an intermediate effect. Plasma lenses in the FRB progenitor host galaxy could be modulating the pulse amplitude as a function of frequency and time (if the source repeats) (Cordes et al. 2017). This effect introduces an additional uncertainty in the FRB rate modeling as the apparent spectral indices of detected FRBs may not be intrinsic. Thus, the observed frequency structure in an FRB (repeating or not) would be dependent on multiple factors including observing frequency, bandwidth, epoch, and even sky direction. If an FRB did occur in the field of view of the telescope while ALFABURST was in operation we could have been unlucky, scintillation or lensing having caused the pulse in the band to go below the detection threshold. Assuming no scintillation or lensing, an increase to the full ALFA band would result in a $\sqrt{6}$ increase in sensitivity compared to what we currently have. But, also important is a more complete sampling of the frequency space if these effects are modulating the pulse.

Macquart & Johnston (2015) conclude that the apparent deficit of FRBs at low Galactic latitudes is due to diffractive interstellar scintillation. Their model shows that the true event rate is a factor of ~ 4 lower than the rate reported in Thornton et al. (2013), which is also the rate used in the standard candle model (Lorimer et al. 2013). The ALFABURST survey is evenly split across high and low Galactic latitudes. Macquart & Johnston (2015) predict that the increase in sensitivity of Arecibo compared to Parkes should result in a factor of 14 increase in detections, assuming a similar bandwidth (~ 300 MHz). Accounting for the smaller bandwidth of ALFABURST means there should still be a factor of a few increase in rates. This non-detection result indicates that the Macquart & Johnston (2015) flux density distribution is not as steep as predicted, or that the source count distribution begins to flatten below the Parkes sensitivity threshold (for further discussion on FRB source counts, see Macquart & Ekers 2017).

The sensitivity of Arecibo allows the ALFABURST survey to probe a search volume out to higher redshifts than other surveys. Our number estimates have assumed that the density of sources per unit co-moving volume is constant. If FRBs are standard candles, and that there is a peak similar to the star formation rate around $z = 2$ (Madau & Dickinson 2014) than the expected event rate that our deeper ALFABURST survey probes would actually be higher than

our simple estimates. Caleb et al. (2016) and Rane (2017) show that a larger sample of FRBs in the Parkes surveys is currently required in order to distinguish between a constant density versus a redshift dependent model. Neglecting other factors that might hinder detection, and keeping in mind the standard candle assumption, our null result suggests that the density of FRBs per unit co-moving volume does not change substantially.

If FRBs are inherently not flat-spectrum sources, then their fluxes will be modified substantially: a steeper negative spectrum population would be harder to detect, while a rising spectrum population would be more readily detectable. Law et al. (2017) report FRB121102 to be band limited during simultaneous observation campaigns using multiple telescopes to cover a broad range of the radio band. Gajjar et al. (2017) observed 15 pulses from FRB121102 across the 4–8 GHz band and reported spectral variation over a brief period of time. A high redshift, band-limited FRB, which ALFABURST is sensitive to, could be shifted below L-band. Such a pulse would not be detected with ALFABURST.

7 CONCLUSIONS AND FUTURE WORK

We have described the implementation and initial operations of a commensal search for transient dispersed pulses using the ALFA receiver on the Arecibo telescope. In our observations carried out so far, we have detected 17 previously known pulsars and found one new high DM transient in the Galactic Plane. Follow-up observations of the same will hopefully reveal the true nature of the source. This serendipitous discovery during a slew shows the importance of developing commensal backends for transient searches on large radio telescopes.

No new FRBs were found in our observations to date. This appears to be broadly consistent with the expectations from a simple model in which FRBs are treated as flat-spectrum standard candles uniformly distributed per unit co-moving volume. We expect continued observations with ALFABURST to run commensally with other ALFA projects, leading to an improvement on the event rate limits of low-fluence FRBs. Quadrupling the current time on-sky, for example, would lead to an expectation of several FRBs and allow us to more quantitatively test the validity of our assumptions about their underlying population, especially the rate dependence on redshift.

The current SPS pipeline is undergoing a significant upgrade. The input bandwidth is limited to 56 MHz of the full 336 MHz digital band due to IO limitations. A new pipeline developed for Square Kilometre Array (SKA) Non-image Processing (NIP) will be used to process the full ALFA band. This will increase sensitivity, and improve detection rates for scintillating or lensed FRBs. An improved version of the real-time RFI exciser is currently being developed and will be deployed to reduce the false detection rate. The post-processing classifier and prioritizer model is being updated to make use of an auto-encoder to select deep features and auto-generate classes. This will allow for an improved follow-up and analysis cycle.

Over the time period ALFABURST has been active, the use of ALFA has decreased as a number of surveys carried out with it have come to an end. We are currently general-

izing the ALFA specific SPS pipeline to be used when other feeds are active. The results from this study would increase our survey time, and sample a larger portion of frequency space.

ACKNOWLEDGEMENTS

We thank the referee for constructive comments on the manuscript. ALFABURST activities are supported by a National Science Foundation (NSF) award AST-1616042. MAM was supported by NSF award number AST-1517003. MPS and DRL were supported by NSF award number OIA-1458952. A.K., J.C., G.F. would like to thank the Leverhulme Trust for supporting this work. G.F., D.M., A.S. acknowledges support from the Breakthrough Listen Initiative. Breakthrough Listen is managed by the Breakthrough Initiatives, sponsored by the Breakthrough Prize Foundation⁶.

REFERENCES

Auld R., et al., 2006, MNRAS, 371, 1617
 Bannister K. W., Madsen G. J., 2014, MNRAS, 440, 353
 Bannister K. W., et al., 2017, ApJ, 841, L12
 Breiman L., 2001, Machine Learning, 45, 5
 Burke-Spolaor S., et al., 2016, ApJ, 826, 223
 Caleb M., Flynn C., Bailes M., Barr E. D., Hunstead R. W., Keane E. F., Ravi V., van Straten W., 2016, MNRAS, 458, 708
 Caleb M., et al., 2017, MNRAS, 468, 3746
 Chawla P., et al., 2017, preprint, ([arXiv:1701.07457](https://arxiv.org/abs/1701.07457))
 Chennamangalam J., et al., 2017, ApJS, 228, 21
 Cordes J. M., Lazio T. J. W., 2002, ArXiv Astrophysics e-prints, Cordes J. M., et al., 2006, ApJ, 637, 446
 Cordes J. M., Wasserman I., Hessels J. W. T., Lazio T. J. W., Chatterjee S., Wharton R. S., 2017, ApJ, 842, 35
 Crawford F., Rane A., Tran L., Rolph K., Lorimer D. R., Ridley J. P., 2016, MNRAS, 460, 3370
 Eatough R. P., Keane E. F., Lyne A. G., 2009, MNRAS, 395, 410
 Farah W., et al., 2017b, Detection of a highly scattered Fast Radio Burst at the Molonglo Radio Telescope, ATel 10867
 Farah W., et al., 2017a, Real-time detection of a Fast Radio Burst at the Molonglo Radio Telescope, ATel 10697
 Gajjar V., et al., 2017, FRB 121102: Detection at 4 - 8 GHz band with Breakthrough Listen backend at Green Bank, ATel 10675
 Heiles C., 2004, Technical Report 2004-11, Accurate Parametric Representation of ALFA Main Beams and First Sidelobes, 1344-1444 MHz. GALFA
 Ho T. K., 1995, in Proceedings of the Third International Conference on Document Analysis and Recognition (Volume 1) - Volume 1. ICDAR '95. IEEE Computer Society, Washington, DC, USA, pp 278-, <http://dl.acm.org/citation.cfm?id=844379.844681>
 Karastergiou A., et al., 2015, MNRAS, 452, 1254
 Keane E. F., Petroff E., 2015, MNRAS, 447, 2852
 Keane E. F., Kramer M., Lyne A. G., Stappers B. W., McLaughlin M. A., 2011, MNRAS, 415, 3065
 Keane E. F., Stappers B. W., Kramer M., Lyne A. G., 2012, MNRAS, 425, L71
 Kohavi R., 1995, in Proceedings of the 14th International Joint Conference on Artificial Intelligence - Volume 2. IJCAI'95. Morgan Kaufmann Publishers Inc., San Francisco, CA, USA, pp 1137-1143, <http://dl.acm.org/citation.cfm?id=1643031.1643047>
 Law C. J., et al., 2017, preprint, ([arXiv:1705.07553](https://arxiv.org/abs/1705.07553))
 Lorimer D. R., Kramer M., 2004, Handbook of Pulsar Astronomy
 Lorimer D. R., Bailes M., McLaughlin M. A., Narkevic D. J., Crawford F., 2007, Science, 318, 777
 Lorimer D. R., Karastergiou A., McLaughlin M. A., Johnston S., 2013, MNRAS, 436, L5
 Macquart J.-P., Ekers R., 2017, preprint, ([arXiv:1710.11493](https://arxiv.org/abs/1710.11493))
 Macquart J.-P., Johnston S., 2015, MNRAS, 451, 3278
 Macquart J.-P., Koay J. Y., 2013, ApJ, 776, 125
 Madau P., Dickinson M., 2014, ARA&A, 52, 415
 Manchester R. N., et al., 2001, MNRAS, 328, 17
 Manchester R. N., Hobbs G. B., Teoh A., Hobbs M., 2005, AJ, 129, 1993
 Marcote B., et al., 2017, ApJ, 834, L8
 Masui K., et al., 2015, Nature, 528, 523
 Pedregosa F., et al., 2011, Journal of Machine Learning Research, 12, 2825
 Petroff E., et al., 2016, Publ. Astron. Soc. Australia, 33, e045
 Rane A., 2017, PhD thesis, West Virginia University
 Scholz P., et al., 2016, ApJ, 833, 177
 Siemion A. P. V., et al., 2012, ApJ, 744, 109
 Spitler L. G., et al., 2014, ApJ, 790, 101
 Spitler L. G., et al., 2016, Nature, 531, 202
 Tendulkar S. P., et al., 2017, ApJ, 834, L7
 Thornton D., et al., 2013, Science, 341, 53
 Tingay S. J., et al., 2015, AJ, 150, 199
 Wagstaff K. L., et al., 2016, PASP, 128, 084503

This paper has been typeset from a *TeX/LaTeX* file prepared by the author.

⁶ breakthroughinitiatives.org